
Low-Energy Atom Scattering from Surfaces

THOMAS ENGEL

Experiments in which low-energy atoms are scattered from surfaces represent an important new method for structural analysis of the topmost atomic layers of a surface. The method and its application in a number of areas in surface science, such as detecting surface defects and studying lattice dynamics, are discussed.

STRUCTURAL STUDIES OF SURFACES HAVE BEEN ONE OF THE main avenues of research in surface science since the 1960's. From chemical studies of gas and liquid phases, investigators have good reason to believe that the way in which atoms are arranged in a molecule is crucial to the properties of the molecule, especially its reactivity. Is structure an equally important factor in considering the properties of solids? The answer is less clear than it is for gases, in which the isolated atoms lack the long-range order characteristic of a solid. Nevertheless, atomic structure is a crucial factor in determining the band structure of semiconductors, metals, and insulators. Electronic devices that make use of the structural arrangement of atoms for a particular element can be fabricated; in this case the bulk structure is the important feature. Geometric structure is also intimately connected with the electronic properties of solids.

The chemical reactivity of solids also depends on the arrangement of atoms, particularly the arrangement in the outermost two to three atomic layers. The reason is that a reaction must take place at the interface between the solid and the second phase, which contains reactants. Studies of catalysis at surfaces [which are discussed in the article by Goodman (1)] show that some catalytically active reactions are greatly accelerated if a particular crystal plane with its characteristic atomic arrangement is exposed to reactants. A striking case of such structural sensitivity for a simple reaction is Pt(100). Here the metastable surface, which has the same structure as would be expected for a continuation of the bulk structure to the surface, adsorbs oxygen 10^3 times more readily than the thermodynamically reconstructed Pt(100) surface (2). The latter is based on a hexagonal symmetry of platinum atoms rather than on the fourfold symmetry characteristic of the normal (100) plane. Many more examples could be cited to show the importance of the surface structure of solids—from the cracking of petroleum to the properties of electronic devices to tribology to battery technology. Much remains to be learned about how the structural arrangement of atoms exposed at a surface can have a profound influence on some processes and a negligible effect on others.

Many techniques have been developed to probe the structure of surfaces. Among the more important of these are scanning tunneling

microscopy, electron microscopy, surface extended x-ray absorption fine structure, ion scattering, surface x-ray diffraction, low-energy electron diffraction (LEED), and diffraction of atomic beams. The first two of these are direct imaging techniques that allow the detection of aperiodic features such as steps and kinks in an otherwise perfectly periodic structure; the others rely on diffraction of waves from a surface. Results obtained with these methods emphasize long-range order, although information about the presence of defects on surfaces can also be obtained with diffraction methods. No single structural technique can cover all the needs of the surface scientist because the information gained through each of these techniques is different. In addition, the possible damage to the surface by the impinging electrons, atoms, or ions must be considered in deciding which of the techniques is best suited for the problem at hand. Finally, no single technique is sufficient to characterize a system completely, so that a structural technique must be compatible with other methods, such as thermal desorption, electron spectroscopies, or adsorption techniques.

The Diffraction of Atoms from Surfaces

The diffraction of helium and molecular hydrogen from a surface formed by cleaving a LiF crystal with a razor blade was first observed in 1930 by Estermann and Stern (3). This experiment was the first to show the wave nature of particles, which had been suggested by de Broglie. In retrospect, it has become clear that Estermann and Stern were astute in the choice of the surface in their experiment. Only a very few materials, such as LiF, MgO, and graphite, are sufficiently inert that the surface periodicity is apparent under the moderate vacuum conditions available in 1930. It was not until ultrahigh vacuum (UHV) techniques were combined with beam sources in 1971 that atom diffraction was observed from a metal surface (4). Results were first obtained from semiconductor surfaces (5) and from adsorbate-covered surfaces (6) in 1979. Since 1930, however, a number of research groups have carried out experiments on inert surfaces that have led to a detailed understanding of the interaction potential between an incident atom or molecule and these surfaces.

To understand the nature of the information obtained from atom diffraction, it is instructive to examine the interaction between an incoming atom or molecule and the surface (Fig. 1). At distances far from the surface, the neutral atom or molecule experiences an attractive potential due to van der Waals forces. As it approaches the surface, the particle experiences a maximum attraction indicated by the potential energy well depth D . If the incident particle can form a chemical bond to the surface, D may be on the order of 1 eV, and the particle will be trapped in the potential. For chemically inert but relatively polarizable atoms such as argon, D is on the order of 80 meV. This interaction is too strong to allow predominantly elastic scattering, and no diffraction is observed. Only if the particle is not

The author is in the Department of Chemistry, University of Washington, Seattle, WA 98195.

too heavy and D is not too large will elastic scattering dominate and diffraction be the most probable scattering event. This has been observed for helium and neon as well as molecular and atomic hydrogen and deuterium scattering from inert surfaces. Typical well depths for helium interacting with a metal surface are on the order of 8 meV.

Of particular importance in understanding the nature of the information contained in atom diffraction is the origin of the repulsive part of the potential shown in Fig. 1. For a closed-shell atom such as helium, it is the overlap of the electron charge density of the atom with those electrons of the solid that penetrate most deeply into the vacuum. This repulsion (V_{rep}), a consequence of the Pauli exclusion principle, can be shown on theoretical grounds (7) to be in general simply related to the total electron charge density, ρ , at the position of the diffracting atom by

$$V_{\text{rep}}(x,y,z) = \alpha \rho(x,y,z) \quad (1)$$

where α is a proportionality constant whose value is 350 eV (atomic unit)³ and where the x and y directions are parallel to the surface and z is normal to the surface. If D is not large, the atom reaches its distance of closest approach to the surface when V_{rep} equals the incident normal energy E_i . This defines a contour above the surface, which forms a diffraction grating for the incident wave. In principle, the distance of closest approach to the surface can be varied by changing E_i . However, because $\rho(x,y,z)$ falls off exponentially with z and because inelastic scattering plays an increasingly important role in the scattering as E_i increases, the classical turning point for most experiments is near 3 Å above the surface plane. The electron charge density at this turning point has values between 1×10^{-4} and 5×10^{-4} (in atomic units), which is several orders of magnitude less than the electron densities in chemical bonds.

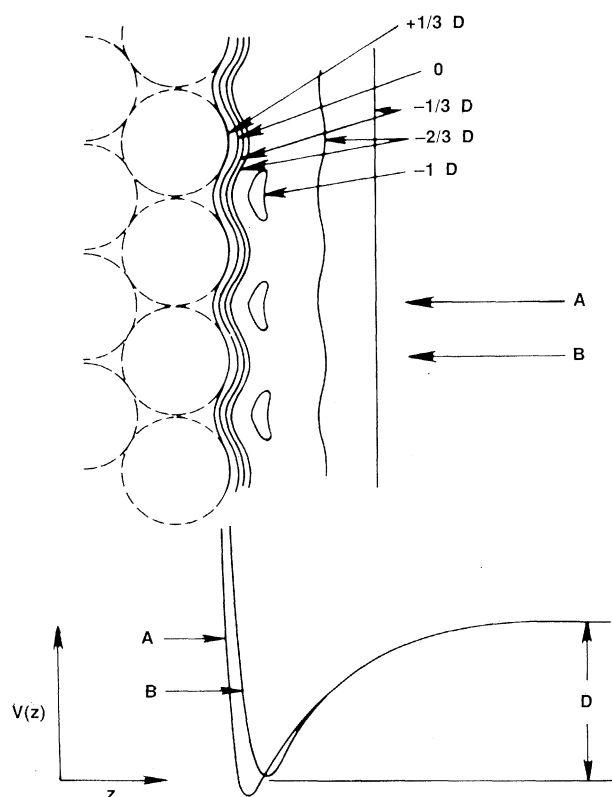


Fig. 1. Interaction of a neutral particle with a solid surface. (Top) Equipotential lines; the negative potential energies are given in fractions of the maximum well depth (D). (Bottom) The potential as a function of z (normal to the surface) for two different impact points (A and B) (28).

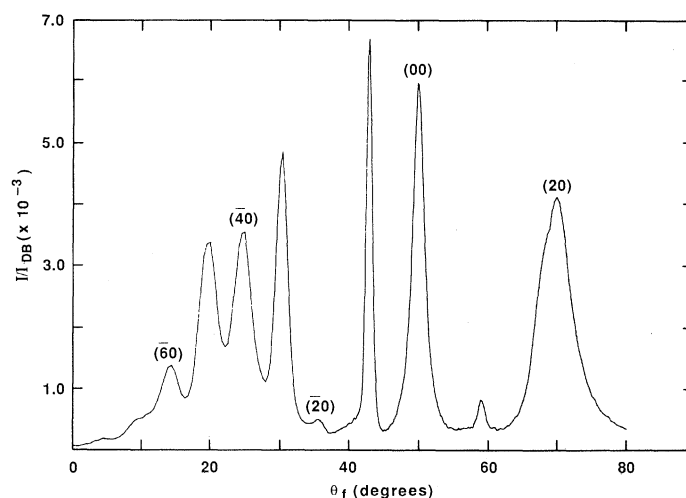


Fig. 2. Normalized diffraction intensity as a function of exit angle (θ_f , measured from the surface normal) for helium scattered from Ni(115). Many well-resolved diffraction peaks are observed. The wavelength of the beam is 0.57 Å (9).

Structural studies that use atom diffraction rely on the fact that the classical turning-point surface, which according to Eq. 1 is a contour of constant charge density, has the periodicity of the surface (Fig. 1). As in any diffraction experiment, the structural information is contained in the relative intensities of the diffraction peaks. Unlike neutron or x-ray diffraction, however, the surface presents continuous scatterers rather than an array of point scatterers. To extract the classical turning-point surface (which is usually referred to as the corrugation function) from experimental data, a model atom-surface potential must be used. Only in very few cases (8) has it been possible to determine an atom-surface potential accurately by means of a combination of diffraction, inelastic scattering, and resonant scattering data. The formulation of a realistic atom-surface potential is an active area of research, and it is clear that the more accurately the potential is known the more structural information that can be extracted from data.

Most structural information obtained from atom scattering experiments has been based on analyses that use a hard-wall potential:

$$V(x,y,z) = 0 \text{ if } z > \zeta(x,y) \\ = \infty \text{ if } z \leq \zeta(x,y) \quad (2)$$

where $\zeta(x,y)$ is the corrugation function. An attractive well can be included in the potential in the form of a refractive index if the finite slope of the repulsive potential shown in Fig. 1 is neglected. An example of a helium diffraction scan obtained from Ni(115) is shown in Fig. 2. For this strongly corrugated surface, many diffraction peaks are seen. A more realistic potential is the corrugated Morse potential given by

$$V(x,y,z) = D \exp \alpha [z - \zeta(x,y)] - 2D \exp \frac{1}{2} \alpha z \quad (3)$$

A detailed comparison of $\zeta(x,y)$ obtained by means of these two very different potentials has been made for helium diffraction from Ni(115) (9). The essential results are that the shape of $\zeta(x,y)$ is the same for either potential but that the amplitude of $\zeta(x,y)$ for the hard-wall potential is 20% larger than for the corrugated Morse potential. This result is encouraging because vastly different potentials yield similar electron density contours. For structural studies, however, in which the goal is to decide between two models that differ only slightly in their atom positions, the atom-surface potential must be well known. This information can be gained through

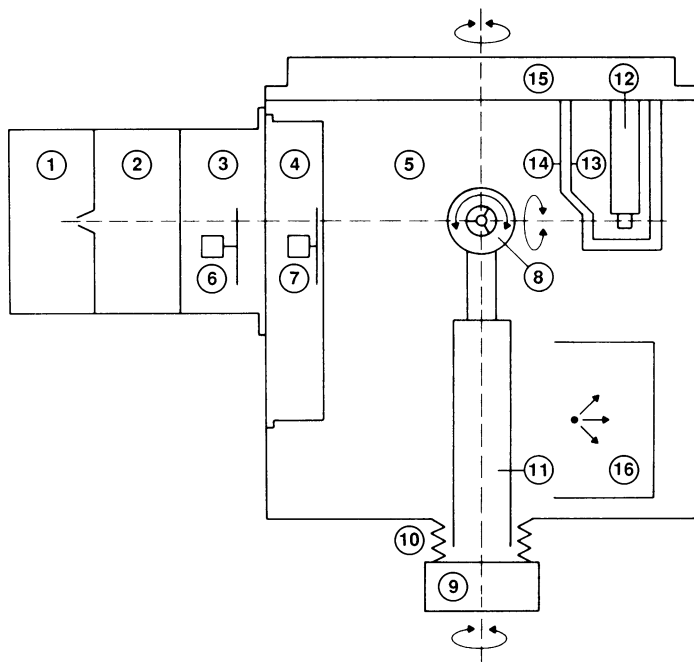


Fig. 3. Schematic drawing of the apparatus used in these studies. (1) Nozzle-skimmer chamber; (2) and (3) first and second differential pumping stages; (4) third differential pumping stage; (5) UHV chamber; (6) 50% duty-cycle chopper; (7) time-of-flight chopper; (8) azimuthal and tilt portions of the sample manipulator; (9) polar axis rotation device; (10) bellows for x - y - z motion; (11) manipulator support cylinder containing liquid nitrogen dewar; (12) quadrupole mass spectrometer detector; (13) and (14) detector differential pumping chambers; (15) rotatable detector flange; (16) titanium sublimation pump (16).

diffraction experiments carried out over a wide range of incident energies and through resonant scattering experiments that probe the attractive region of the potential.

The determination of the corrugation function is only half the structural problem. The experimentally determined quantity is the contour of charge density corresponding to approximately 10^{-4} in atomic units. The desired information is the position of the atoms at the surface. Therefore, a structural analysis involves calculating the electron density contour at a density appropriate for the incident energy and a given set of atom positions and then comparing it with the experimentally determined corrugation function. This step is currently the weakest link in the chain of processes needed for quantitative structural analyses by means of atom diffraction. Methods to generate electron density contours range in complexity from isolated atom superposition (10) to self-consistent solid-state methods (11). Various elements of the problems inherent in calculating density contours at low values have been discussed (12); it is to be expected that, as more diffraction experiments are carried out on a variety of surfaces, advances in the theory will follow.

Even though quantitative crystallographic determinations done by means of atom diffraction are limited by incomplete understanding of the atom-surface potential, there are many research areas that can be pursued with our present knowledge. These include choosing between different structural models proposed for the same surface (13), studying phase transitions at surfaces (14), detecting defects such as steps and kinks on surfaces (15), identifying roughening transitions on metal surfaces (16), studying changes in surface topography induced by sputtering (17), and studying surface diffusion (18). These areas involve only elastic scattering of atoms from surfaces. Additional studies of energy transfer between helium atoms and surfaces have given important insight into lattice vibra-

tions and force constants between surface atoms. This extends the applicability of atom-scattering techniques to a wide range of problems dealing with lattice dynamics.

Experimental Considerations

Structural studies on reactive surfaces require vacua on the order of 10^{-10} torr to prevent residual gases in the vacuum system from contaminating the surface in a short time. For atom diffraction studies, a beam source must be coupled to the UHV scattering chamber in which the sample is mounted.

The complexity of an atom diffraction experiment can best be illustrated by comparing it with a LEED experiment. In the case of LEED, a hot filament is the source of electrons, which can be collimated, accelerated, and focused onto the sample with electrical potentials applied to elements of an electron gun. After diffraction from the surface, the electrons in the discrete beams pass through a field-free space, after which they are energy-selected by means of hemispherical grids and accelerated onto a fluorescent screen. The light intensity, which is proportional to the diffraction intensity, can be recorded from outside the vacuum chamber with a video camera. For atom diffraction, sources are more complex because neutral atoms cannot be focused. The atom beam is generated by expansion of a gas at high pressure (10 to 100 atmospheres) through an orifice

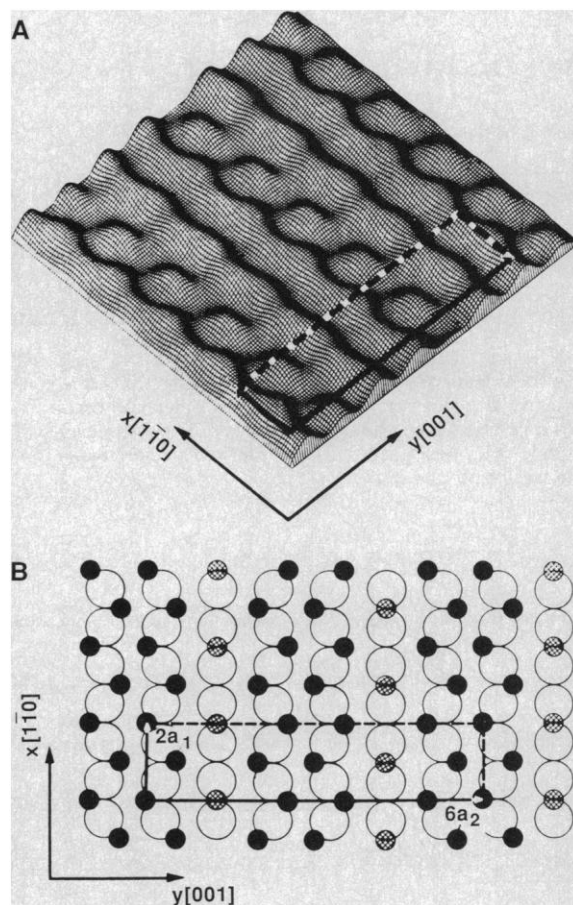


Fig. 4. (A) The corrugation function determined from helium diffraction from a Ni(110) surface covered with 0.8 monolayer of hydrogen atoms. (B) A structural model consistent with the experimental results. The small dark and cross-hatched circles correspond to hydrogen bound at two different types of sites, and the large open circles corresponding to the topmost layer of nickel atoms (25).

whose diameter is on the order of 0.02 mm. Gas emerges into the vacuum in front of the nozzle in a broad cone of exit angles, and apertures are used to select a small range of exit angles corresponding to trajectories perpendicular to the nozzle plane. Only roughly 1 in 10^6 atoms that leave the nozzle strikes the sample; the rest must be pumped away for compatibility with the UHV conditions in the scattering chamber. The space between successive collimating apertures is pumped separately to ensure that this occurs.

The expansion of the gas as it passes from the nozzle into the vacuum is a crucial aspect of the generation of an atom beam suitable for diffraction from surfaces. As the gas expands into the vacuum, collisions between atoms lead to a narrowing of the velocity distribution, so that the spread in velocities about the mean drift velocity can be made as narrow as that which would be achieved in an equilibrium gas at 10^{-2} K (19). This narrowing of the velocity distribution is critical because otherwise the beam would contain a spread of wavelengths that would smear the diffraction peaks.

Finally, detecting the diffracted particles is more difficult than in LEED because simple displays, such as a phosphorescent screen, cannot be used to image neutral atoms of an inert gas. Most atom diffraction studies use a mass spectrometer as a detector, although bolometers have also been used. Because the angular distribution of the backscattered particles must be measured, the mass spectrometer

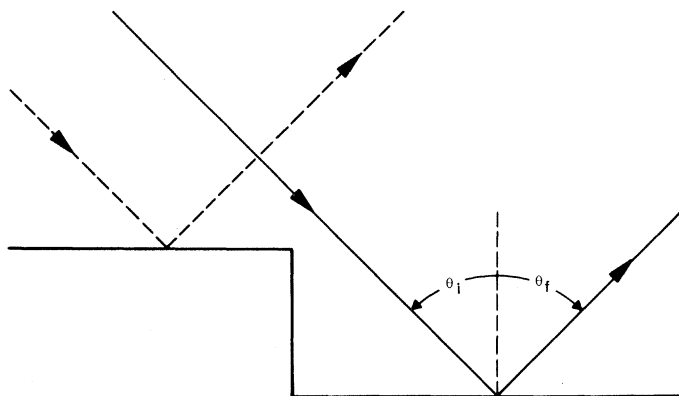


Fig. 5. Schematic illustration of interference obtained in scattering from a surface in the vicinity of a step edge. Whether the interference is constructive or destructive depends on whether the path difference between the two indicated trajectories is an odd or even number of half wavelengths. θ_i and θ_f are the angle of incidence and the scattering angle, respectively, as measured from the surface normal.

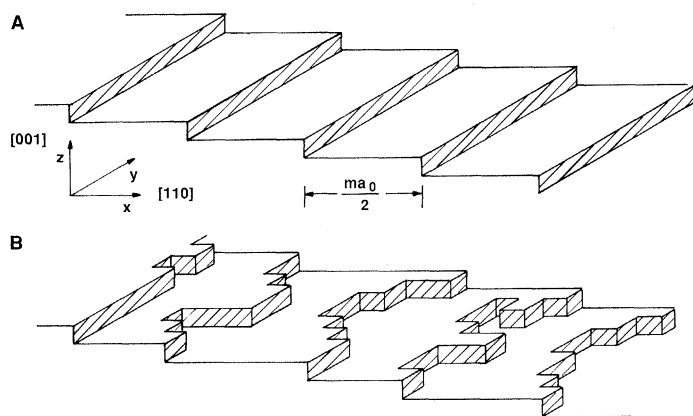


Fig. 6. Idealized view of a stepped metal surface. These consist in general of relatively close-packed terraces separated by a step that is one atomic spacing high. (A) The configuration present at low temperatures. (B) The configuration expected above the transition temperature to the rough state (16).

must be rotated about the scattering center without compromising the UHV environment. Furthermore, the detector is best placed in its own vacuum chamber with collimating apertures that view only the impact point of the beam on the surface. In this way the detector will not measure the pressure rise in the scattering chamber that is due to the beam flux equilibrating with the chamber walls. Because the measurement of the intensity of the diffraction beams requires that the detector sample as much as possible of the half-space in front of the single crystal sample, suitable rotations of the detector and sample must be incorporated into the design. A single rotation of the detector in the scattering plane coupled with separate polar, tilt, and azimuthal sample rotations, or two detector and two sample rotation modes, will enable the half-space to be scanned.

Figure 3 shows schematically the apparatus used in our laboratory for atom diffraction studies (16). By means of two-stage differential pumping of the detector and synchronous detection, a sensitivity of 1 part in 10^5 of the incident beam intensity can be achieved in a counting time of several seconds. In this apparatus, four differentially pumped stages are used in the beam-generating portion, and the detector can be rotated in the scattering plane. The sample is mounted on a three-axis manipulator (20), which allows cooling to 90 K and heating to high temperatures by electron bombardment of the sample.

Although such an apparatus is highly complex, its versatility is great. The same apparatus can be used to study lattice dynamics of clean and adsorbate-covered surfaces by measuring the energy transferred between the impinging gas atoms and the bulk and surface phonons of the substrate. Furthermore, with slight modifications, an atom diffraction apparatus can be used to study chemical reactions on surfaces. This is particularly useful when the reactants are highly reactive, because a molecular beam confines the reactants to collisions with the sample, thereby eliminating spurious wall

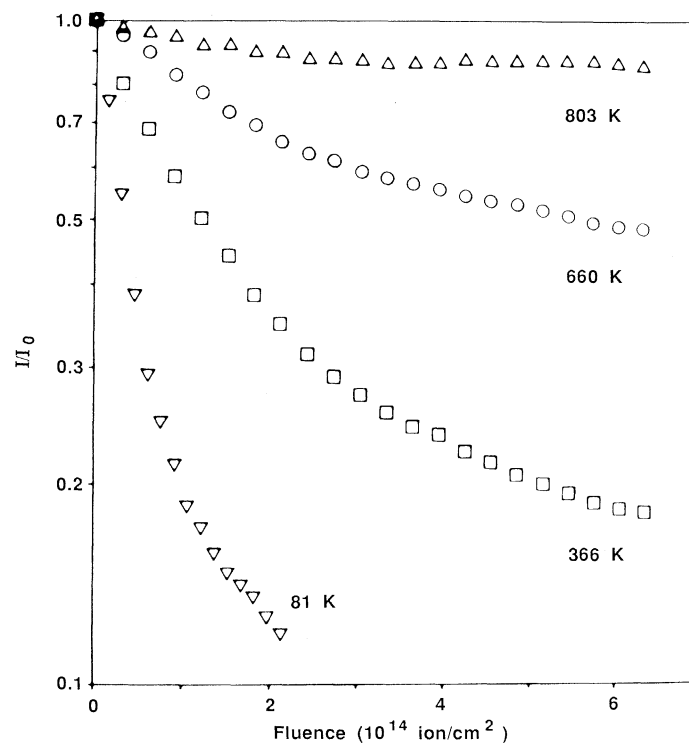


Fig. 7. Ratio of the specular intensity after ion bombardment to that from a defect-free surface as a function of the number of ions that have struck the surface. Because of the large cross section of the defect produced, helium atoms are scattered into a diffuse background, which leads to a strong attenuation of the specular peak (17).

effects. With the use of relaxation techniques (21), fast reaction kinetics can be studied on surfaces; such studies have led to the unambiguous determination of reaction mechanisms for a number of catalytically important reactions.

Applications of Atom Scattering from Surfaces

Atom scattering, particularly helium scattering, has been useful in structural determinations, surface diffusion studies, surface defect detection, phase transition experiments, and lattice dynamics studies (22-24). In all these applications, details of the atom-surface potential are of minor importance; thus the technique can be used to its full advantage without this information.

Atom scattering is well suited for studies involving hydrogen adlayers. Of all adsorbates, hydrogen is perhaps the most important because it is a reactant in many catalytic processes, such as petroleum refining. Since hydrogen atoms are weak electron scatterers, LEED has been only minimally useful in determining lattice positions occupied by hydrogen. Because the classical turning point of diffracting helium atoms occurs at a low electron density, however, helium is sensitive to lattice atoms of both low and high atomic number.

One example of an atom scattering experiment involving hydrogen adlayers (25) has shown that a number of phases of hydrogen are formed on Ni(110), depending on the surface coverage. Figure 4 shows an experimentally determined corrugation surface for a hydrogen coverage of 0.8 monolayer as well as a structural model consistent with the experimental data. The electrons localized at the adsorbed hydrogen atoms push the contour of constant electron charge density further into the vacuum, giving rise to maxima at the

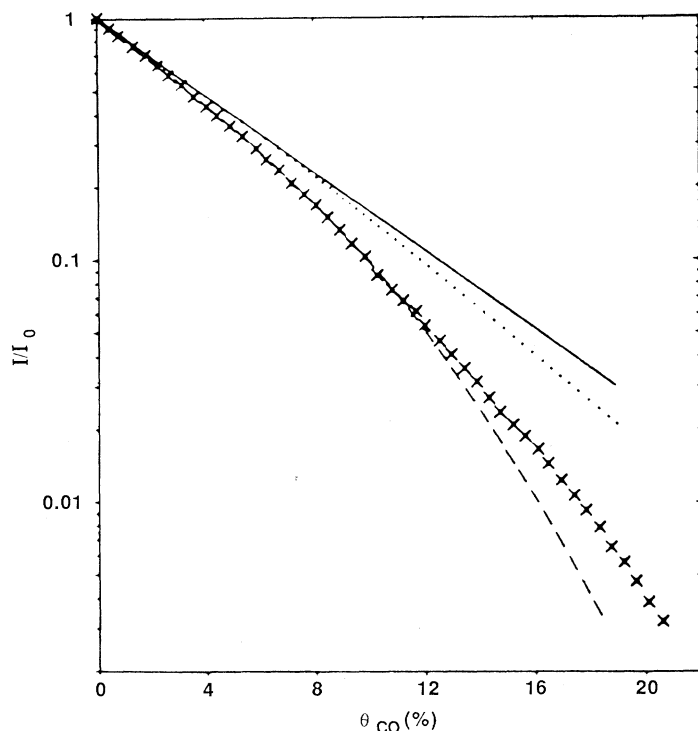


Fig. 8. Ratio of the specular intensity after CO adsorption to that from a CO-free surface as a function of the CO coverage. Data were obtained on a Pt(111) surface with $E_i = 63$ meV. (x) Experimental data; the three lines represent the behavior expected for different models. The dotted line is for a lattice gas of CO molecules; the dashed line is for a lattice gas in which nearest neighbor sites are excluded (26).

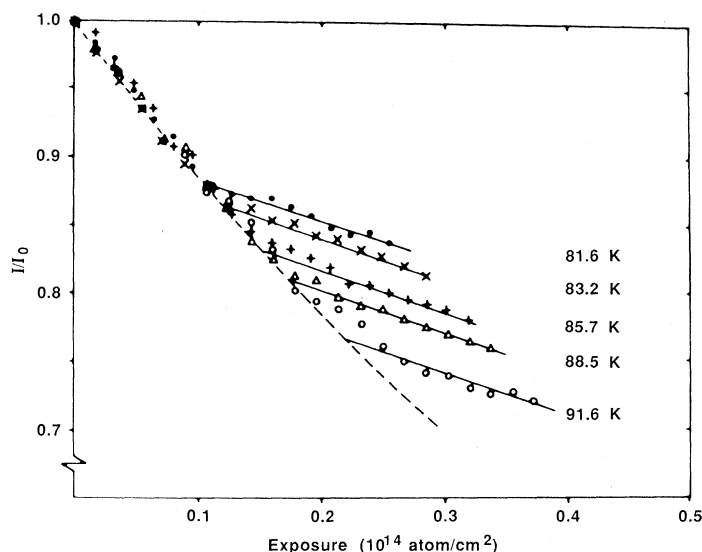


Fig. 9. Ratio of the specular intensity at a given xenon coverage to that for the clean surface as a function of the number of xenon atoms that have struck the surface. For low exposures, the helium beam is greatly attenuated because the xenon atoms are randomly distributed on the surface. At a coverage corresponding to condensation of this lattice gas into well-ordered islands, the attenuation decreases because most of the scattering into the diffuse background (which leads to attenuation) is due to atoms at the island edges only (29).

position of the underlying atoms. The resulting structure appears to be complex, but it is actually determined by two competing forces: repulsive interactions in the adlayer, which try to arrange the adatoms in a hexagonal lattice, and attractive forces between adatoms and the surface atoms, which try to maintain registry between the adlayer and the substrate. The structure represents a compromise between these two factors. Without accurate atom-surface potentials and charge density calculations, atom-surface spacings cannot be determined; however, Fig. 4 does show certain aspects of the structure. At present, most of our understanding of the atomic arrangement of hydrogen adlayers on various metal surfaces comes from atom diffraction experiments.

Although diffraction experiments emphasize the long-range order aspects of surfaces, aperiodic features such as surface kinks or steps are equally important because they can have a significant effect on reaction kinetics at surfaces. Atom diffraction is ideally suited to probe the defect structure at surfaces because of the attractive part of the atom-surface potential. As in the gas phase, this gives rise to scattering for large impact parameters. Therefore, vacancies or kinks have scattering cross sections on the order of 100 to 200 \AA^2 , which is many times their geometric size (26). This means that even a few defects can significantly affect scattering intensities.

Figure 5 shows a two-level system that would result locally on a surface if steps were created on it through sputtering or thermal activation. For specular scattering, in which the incident and reflected angles are equal, there are two characteristic sets of angles. For one set, the path difference for scattering from the two levels is an integral number of wavelengths. These correspond to in-phase scattering from the two levels, and the scattered intensity is identical to that if no steps were present. The second set of angles corresponds to trajectories in which the path difference between scattering from the two levels is an odd number of half wavelengths. This leads to destructive interference. For this antiphase condition, the specular peak is broadened and the maximum intensity reduced.

This characteristic diffraction beam broadening and intensity reduction under antiphase conditions, which is a unique signature of

steps on surfaces, has been used to establish the existence of a roughening transition on metal surfaces (16). For a surface that is inclined with respect to a relatively close-packed plane of low surface energy, the equilibrium configuration at very low temperatures is that shown in Fig. 6A. The low surface energy terraces are separated by steps that are one atomic spacing high. Above a critical temperature, the surface assumes the configuration shown in Fig. 6B, in which the step edges meander. The meandering is unbounded for an infinitely large single crystal, leading to the surprising result that the surface is no longer well defined. This result is of course modified for real surfaces, for which coherent domain sizes are generally only on the order of 1000 Å. The meandering of the step edge that is bounded for finite domain sizes, however, will generate kink sites of high coordination number; this phenomenon may be of importance in reactions on supported catalysts that generally exhibit appreciable areas of high-index planes. Recent experiments indicate that the transition temperature to the rough state is 450 K for Ni(115) (16), where the terrace width is 6.5 Å, and 750 K for Ni(113) (27), where the terrace width is 3.9 Å. Because such temperatures are not outside the range used in the catalytic industry, these insights into the equilibrium configuration of high-index crystal planes may be of importance in understanding reactions on surfaces.

If a well-ordered single crystal surface is bombarded with argon ions at low temperatures in the process called sputtering, random

defects are produced. Because of the large scattering cross section associated with the defect, the specular scattering for a helium beam is strongly attenuated. If the same process is carried out at higher temperatures, at which surface diffusion can anneal the defects, the attenuation of the specular scattering is reduced (Fig. 7). From measurements of this type, absolute sputtering yields and rates of surface diffusion can be determined (17). Thus important technical questions can be addressed without a complex analysis of the data.

The degree to which the specular beam is attenuated by individual surface scatterers on an otherwise well-ordered surface gives an indication of how the scatterers are distributed. This applies whether the scatterers are vacancies or adatoms, as illustrated in Fig. 8. Here the specular helium beam is attenuated by adsorbed CO molecules; the intensity is reduced by an order of magnitude by 5% of a monolayer of CO. The exact form of the attenuation depends on whether the adatom interaction leads to ordering; for this particular case adsorption is consistent with the exclusion of nearest neighbor sites, showing that adjacent CO molecules strongly repel one another.

Above a critical coverage, the adsorbed gas condenses into well-ordered islands as a result of attractive forces, and the attenuation is less than that for a random distribution at the same coverage. This abrupt change in attenuation as coverage is increased can be used to identify a surface phase transition from a disordered gas to a two-dimensional solid. By mapping the coverage at which this occurs for various temperatures (Fig. 9), the phase diagram for the two-dimensional system can be determined.

The preceding examples were taken from studies in which the elastic intensity was measured after atom scattering from the surface. By introducing a chopper into the beam line with a narrow slit, pulses of atoms with widths on the order of 10^{-5} second can strike the surface. By measuring their time of flight to the detector, the energy lost to or gained from the surface phonons can be determined. By making these measurements for various scattering angles, the dispersion relation between the energy of the phonon mode and its wavelength can be determined. Figure 10 shows results obtained for krypton films. Monolayer films do not show dispersion, indicating that individual atoms vibrate completely independently of one another; thicker films do exhibit dispersion, showing that collective modes of the adlayer are excited by the collision with the helium atom. Such studies can be used to determine the force constants linking neighboring surface atoms and can thereby enhance our understanding of the stability of surfaces. They can also provide a microscopic picture of the driving force behind phase transitions at surfaces.

Conclusions

This survey of atom scattering from surfaces has covered only a small portion of current research. Major insights into fundamental areas, such as the atomic structure of adlayers and the existence of certain classes of phase transitions, have become possible through the use of atom scattering techniques. In addition, solutions to problems of a more technical nature, such as surface diffusion and the determination of sputtering yields, have been possible by using the large cross sections associated with vacancies and adatoms on surfaces. Because a modern surface scattering apparatus can be used to carry out all these experiments, to study lattice dynamics through inelastic scattering measurements, and to determine the mechanisms of surface reactions by means of relaxation techniques, a large span of surface science can be covered. With the advances that have been made in the field in the last decade, we can be optimistic about what the next decade will bring.

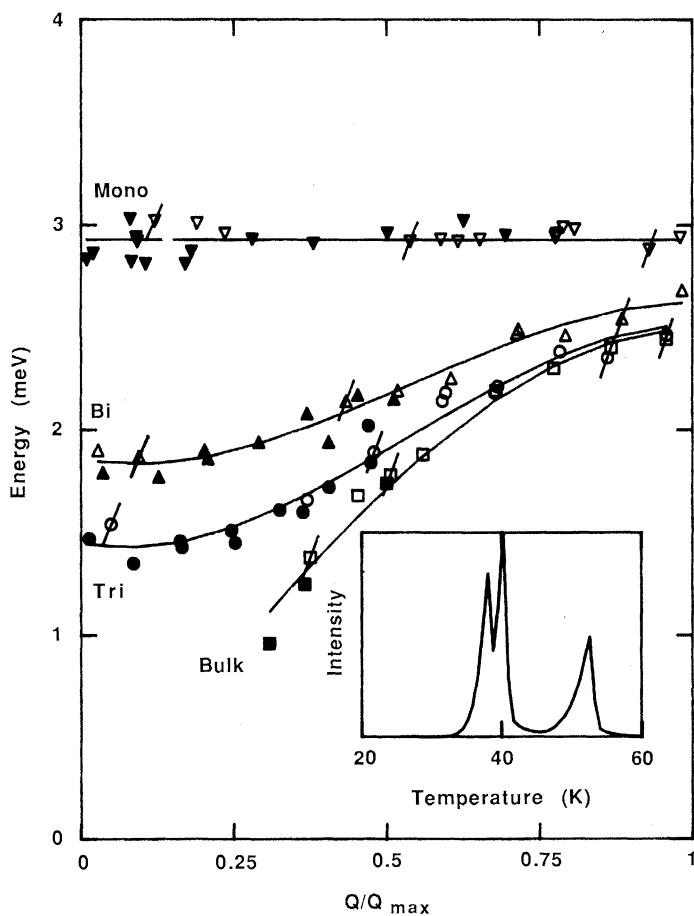


Fig. 10. Phonon dispersion curves for mono-, bi-, and trilayers of krypton atoms on a Ag(111) surface. The characteristic variation of the phonon energy with the wave vector of excitation (Q) is different for different film thicknesses. This shows the complexity of lattice dynamics for adsorbed layers. (Inset) A thermal desorption spectrum from a trilayer film. The monolayer is desorbed at the highest temperature because it is most strongly bound to the surface. The third layer desorbs at a lower temperature than the second, as can be seen in the two peaks near 40 K (30).

REFERENCES AND NOTES

1. W. Goodman, *Science*, in press.
2. G. Pirug, G. Broden, H. P. Bonzel, in *Proceedings of the Seventh International Vacuum Congress and the Third International Conference on Solid Surfaces*, R. Dobrozemsky, F. Rüdener, F. P. Viehböck, A. Breth, Eds. (R. Dobrozemsky et al., Vienna, 1977), p. 907.
3. J. Estermann and O. Stern, *Z. Phys.* **61**, 95 (1930).
4. D. V. Tendulkar and R. E. Stickney, *Surf. Sci.* **27**, 516 (1971).
5. M. J. Cardillo and G. E. Becker, *Phys. Rev. Lett.* **42**, 508 (1979).
6. K. H. Rieder and T. Engel, *ibid.* **43**, 373 (1979).
7. M. Manninen et al., *Phys. Rev. B* **29**, 2314 (1984).
8. V. Celli, D. Eichenauer, A. Kaufhold, J. P. Toennies, *ibid.* **32**, 5044 (1985).
9. D. S. Kaufman, R. M. Aten, E. H. Conrad, L. R. Allen, T. Engel, in preparation.
10. D. Haneman and R. Haydock, *J. Vac. Sci. Technol.* **21**, 330 (1982).
11. D. R. Hamann, *Phys. Rev. Lett.* **46**, 1227 (1981).
12. J. Tersoff, M. J. Cardillo, D. R. Hamann, *Phys. Rev. B* **32**, 5044 (1985).
13. M. J. Cardillo et al., *ibid.* **28**, 494 (1983).
14. K. Kern, R. David, R. L. Palmer, G. Comsa, *Phys. Rev. Lett.* **56**, 620 (1986).
15. L. J. Gomez, S. Bourgeat, J. Ibanez, M. Salmeron, *Phys. Rev. B* **31**, 2551 (1985).
16. E. H. Conrad et al., *J. Chem. Phys.* **84**, 1015 (1986). See also an erratum to this paper (*ibid.*, in press).
17. B. Poelsma, L. K. Verheij, G. Comsa, *Phys. Rev. Lett.* **53**, 2500 (1984).
18. ———, *ibid.* **49**, 1731 (1982).
19. J. P. Toennies and K. Winkelmann, *J. Chem. Phys.* **66**, 3965 (1977).
20. T. Engel, D. Braid, E. H. Conrad, *Rev. Sci. Instrum.* **57**, 487 (1986).
21. M. P. D'Evelyn and R. J. Madix, *Surf. Sci. Rep.* **3**, 413 (1983).
22. T. Engel and K. H. Rieder, *Springer Tracts in Modern Physics* (Springer-Verlag, Berlin, 1982), vol. 91.
23. K. H. Rieder, *Contemp. Phys.* **26**, 559 (1985).
24. J. A. Barker and D. J. Auerbach, *Surf. Sci. Rep.* **4**, 1 (1984).
25. T. Engel and K. H. Rieder, *Surf. Sci.* **109**, 140 (1981).
26. B. Poelsma and G. Comsa, *Faraday Discuss. Chem. Soc.* **80** (no. 16) 1 (1985).
27. E. H. Conrad, L. R. Allen, D. Blanchard, T. Engel, in preparation.
28. J. P. Toennies, *Appl. Phys.* **3**, 91 (1974).
29. B. Poelsma, L. K. Verheij, G. Comsa, *Phys. Rev. Lett.* **51**, 2410 (1983).
30. K. D. Gibson and S. J. Sibener, *ibid.* **55**, 1514 (1985).

Polarized Electron Probes of Magnetic Surfaces

ROBERT J. CELOTTA AND DANIEL T. PIERCE

The magnetic properties of surfaces are now being explored with electron spectroscopies that use electron spin polarization techniques. The increased activity in surface magnetic measurements with polarized electron beams is spurred by new scientific and technological challenges and is made feasible by recent advances in the technology of sources and detectors of polarized electrons. The ability to grow thin films and to engineer artificial structures permits new phenomena to be investigated at magnetic surfaces and interfaces. For such investigations, spin-polarized electron techniques—such as polarized electron scattering, polarized photoemission, polarized Auger spectroscopy, and scanning electron microscopy with polarization analysis—have been and will probably continue to be used to great advantage.

MUCH OF WHAT WE KNOW ABOUT SURFACES ON THE atomic level comes from electron-based measurements. Our knowledge of microstructures in general is largely a consequence of rapid advancement in the field of electron microscopy. It is therefore surprising that use has not been made of the full information content of an electron beam, in particular the degree of electron spin polarization.

Electron-based measurements typically determine the change in momentum of an incident probing electron, the momentum distribution of emitted electrons, or, in the case of the scanning electron microscope, simply the number of emitted electrons. Since 1925, however, it has been known (1) that each electron possesses a spin, with an associated magnetic dipole moment having a fixed strength and variable orientation in space. It is this additional degree of freedom, the orientation of the electron spin, that is the key to obtaining more information about the system under study.

A fully characterized electron beam has either been prepared with or measured to have a specific momentum and polarization. The polarization of an electron beam in the z direction is defined as

$$P_z = \frac{N_{\uparrow} - N_{\downarrow}}{N_{\uparrow} + N_{\downarrow}} \quad (1)$$

where N_{\uparrow} (or N_{\downarrow}) represents the number of electron spins parallel (or antiparallel) to the z direction. A completely polarized electron beam has a polarization vector magnitude of unity, compared to an "ordinary" beam with a polarization of zero.

Macroscopic fields, such as those used to separate atoms of differing spins in a Stern-Gerlach experiment, cannot be used (2) with free electrons to filter out those electrons with a particular spin direction to form a highly polarized beam. While many clever ways (2) of producing and detecting electron polarization have been suggested during the last 50 years, only recently have polarized electron sources and detectors progressed to the stage where they may be used routinely in experiments. This accounts in large measure for the relative paucity of experimental results in the field.

Measurement of the polarization of an electron beam makes it possible to learn more about systems in which interactions affecting the spin of the electron occur. The spin-orbit and exchange interactions do this in fundamentally different ways. In the spin-orbit interaction, the magnetic dipole of the incident electron interacts with the electric field of an atom in the sample. This is a relativistic effect that is largest for heavy atoms and can cause a redistribution of the direction of the spins, that is, a change in the polarization. The exchange interaction comes about as a consequence of the Pauli exclusion principle, which forbids any two electrons from having exactly the same quantum numbers. Hence, the spatial part of the wave function of two colliding electrons with the same spin direction will be different from that of two electrons with opposite

The authors are in the Radiation Physics Division at the National Bureau of Standards, Gaithersburg, MD 20899.